Title

The N-terminal tail of C. elegans CENP-A interacts with KNL-2 and is essential for centromeric chromatin assembly

Journal

Molecular Biology of the Cell, 32(12)

ISSN

1059-1524

Authors

de Groot, Christian
Houston, Jack
Davis, Bethany
et al.

Publication Date

2021-06-01

DOI

10.1091/mbc.e20-12-0798

Peer reviewed

The N-terminal tail of *C. elegans* CENP-A interacts with KNL-2 and is essential for centromeric chromatin assembly

Christian de Groot[a,b,†], Jack Houston[a,†], Bethany Davis[a,b,c], Adina Gerson-Gurwitz[a,b], Joost Monen[a,d], Pablo Lara-Gonzalez[a], Karen Oegema[a,e,f], Andrew K. Shiau[b,e], and Arshad Desai[a,e,f,*]

[a]Ludwig Institute for Cancer Research, San Diego Branch, La Jolla, CA 92093; [b]Small Molecule Discovery Program, Ludwig Institute for Cancer Research, La Jolla, CA 92093; [c]Department of Biology and Chemistry, Embry-Riddle Aeronautical University, Prescott, AZ 86301; [d]School of Theoretical & Applied Science, Ramapo College of New Jersey, Mahwah, NJ 07430; [e]Section of Cell & Developmental Biology, Division of Biological Sciences and [f]Department of Cellular & Molecular Medicine, University of California San Diego, La Jolla, CA 92093

ABSTRACT **Centromeres are epigenetically defined by the centromere-specific histone H3 variant CENP-A. Specialized loading machinery, including the histone chaperone HJURP/Scm3, participates in CENP-A nucleosome assembly. However, Scm3/HJURP is missing from multiple lineages, including nematodes, with CENP-A-dependent centromeres. Here, we show that the extended N-terminal tail of *Caenorhabditis elegans* CENP-A contains a predicted structured region that is essential for centromeric chromatin assembly; removal of this region prevents CENP-A loading, resulting in failure of kinetochore assembly and defective chromosome condensation. By contrast, the N-tail mutant CENP-A localizes normally in the presence of endogenous CENP-A. The portion of the N-tail containing the predicted structured region binds to KNL-2, a conserved SANTA domain and Myb domain-containing protein (referred to as M18BP1 in vertebrates) specifically involved in CENP-A chromatin assembly. This direct interaction is conserved in the related nematode *Caenorhabditis briggsae*, despite divergence of the N-tail and KNL-2 primary sequences. Thus, the extended N-tail of CENP-A is essential for CENP-A chromatin assembly in *C. elegans* and partially substitutes for the function of Scm3/HJURP, in that it mediates a direct interaction between CENP-A and KNL-2. These results highlight an evolutionary variation on centromeric chromatin assembly in the absence of a dedicated CENP-A–specific chaperone/targeting factor of the Scm3/HJURP family.**

Monitoring Editor
Kerry Bloom
University of North Carolina, Chapel Hill

Received: Dec 28, 2020
Revised: Apr 6, 2021
Accepted: Apr 7, 2021

INTRODUCTION

Centromeres are specialized chromosomal loci that direct chromosome segregation. In most species, active centromeres are defined by the presence of CENP-A, a histone variant that replaces histone H3 in centromeric nucleosomes (Kixmoeller *et al.*, 2020; Mitra *et al.*, 2020). CENP-A provides the physical foundation for assembly of the kinetochore, a multiprotein complex mediating spindle microtubule attachment to chromosomes (Musacchio and Desai, 2017). The cues leading to the centromere-restricted localization of CENP-A are being actively investigated. The underlying centromeric DNA is not conserved and, with the exception of budding yeasts, neither necessary nor sufficient to propagate CENP-A chromatin (Allshire and Karpen, 2008; McKinley and Cheeseman, 2016).

A segment of the histone fold domain of CENP-A, known as the CENP-A targeting domain (CATD), when transferred into canonical histone H3, is sufficient to confer centromere localization (Black *et al.*, 2004). The CATD of CENP-A interacts with a CENP-A–specific histone chaperone, known as Holliday junction repair protein (HJURP) in vertebrates and Scm3 in fungi (Dunleavy *et al.*, 2009; Foltz *et al.*, 2009). This interaction is essential for CENP-A centromere

This article was published online ahead of print in MBoC in Press (http://www.molbiolcell.org/cgi/doi/10.1091/mbc.E20-12-0798) on April 14, 2021.

†These are co-first authors.

*Address correspondence to: Arshad Desai (abdesai@ucsd.edu).

Abbreviations used:

targeting during mitotic exit (Jansen *et al.*, 2007; Foltz *et al.*, 2009). However, HJURP/Scm3 is not conserved in all species that build centromeres using CENP-A, including insects and nematodes (McKinley and Cheeseman, 2016). In *Drosophila melanogaster,* there is compelling evidence that the unrelated protein Cal1 acts as a functional homologue of HJURP/Scm3 (Erhardt *et al.*, 2008; Mellone *et al.*, 2011; Chen *et al.*, 2014). By contrast, in *C. elegans,* no HJURP/Scm3-like activity has been identified to date.

In addition to promoting CENP-A nucleosome assembly, HJURP/Scm3 proteins target the CENP-A/H4-HJURP/Scm3 prenucleosomal complex to the specific location of the centromere by interaction with centromeric DNA/chromatin-bound targeting factors. In budding yeast, the CBF3 complex specifically recognizes centromeric DNA and its subunit Ndc10 interacts with HJURP/Scm3 of the prenucleosomal complex to localize new CENP-A nucleosome assembly (Cho and Harrison, 2011). Outside of budding yeasts, where the CBF3 complex is not present, the Mis18 complex is the primary candidate for recognizing existing centromeric chromatin domains and targeting the deposition of new CENP-A via an interaction with HJURP/Scm3. The Mis18 complex is composed of Mis18 and/or KNL-2/M18BP1, depending on the species: Mis18α, Mis18β, and M18BP1 in humans (Fujita *et al.*, 2007); Mis18 only in *Schizosaccharomyces pombe* (Hayashi *et al.*, 2004; Pidoux *et al.*, 2009; Williams *et al.*, 2009); KNL-2 only in *C. elegans* (Maddox *et al.*, 2007), and *Arabidopsis* (Lermontova *et al.*, 2013). *S. pombe* Mis18 and human Mis18α/β interact with HJURP/Scm3 in vitro (Pidoux *et al.*, 2009; Wang *et al.*, 2014; Nardi *et al.*, 2016; Pan *et al.*, 2019) and Mis18 complex-mediated CENP-A recruitment can be bypassed by artificial tethering of HJURP/Scm3 to chromatin (Foltz *et al.*, 2009; Barnhart *et al.*, 2011; Ohzeki *et al.*, 2012). In human cells, centromere localization of the Mis18 complex precedes that of the CENP-A-H4-HJURP prenucleosomal complex during mitotic exit-coupled new CENP-A chromatin assembly (Jansen *et al.*, 2007). The Mis18 complex is proposed to recognize existing centromeric chromatin at least in part by binding to CENP-C, the reader of CENP-A nucleosomes that directs kinetochore assembly (Moree *et al.*, 2011; Kato *et al.*, 2013). However, in *C. elegans*, KNL-2 localizes to chromatin independently of CENP-C (Maddox *et al.*, 2007) and, even in nonmammalian vertebrates, the Mis18 complex directly recognizes CENP-A nucleosomes (French *et al.*, 2017; Hori *et al.*, 2017). KNL-2/M18BP1 family proteins contain a conserved Myb-like DNA-binding domain and a SANTA domain whose functions independent of CENP-C association are unclear (Zhang *et al.*, 2006; Maddox *et al.*, 2007; Ohzeki *et al.*, 2012; French and Straight, 2019). Interestingly, in fungi where KNL-2/M18BP1 proteins are absent, Myb domains can be found in HJURP/Scm3 proteins (Sanchez-Pulido *et al.*, 2009), suggesting potential fusion of multiple functions within a single polypeptide.

Here, we investigate CENP-A chromatin in *C. elegans,* which requires KNL-2/M18BP1 for its assembly but lacks an HJURP/Scm3 family member. *C. elegans* is holocentric, with condensed mitotic chromosomes having two "stripes" of CENP-A chromatin—one per sister chromatid—on geometrically opposite surfaces (Maddox *et al.*, 2007; Melters *et al.*, 2012). Genomic approaches have localized CENP-A and KNL-2 to broad permissive domains in the *C. elegans* genome that are transcriptionally inactive (Gassmann *et al.*, 2012), although restriction to specific sites has also been suggested (Steiner and Henikoff, 2014). We focused on the unusually long amino-terminal tail (N-tail) of *C. elegans* CENP-A, which, unlike the N-termini of CENP-A from other species, is predicted to harbor a region with α-helical secondary structure. Analysis of the divergent N-tails of CENP-A family members have implicated them in kinetochore assembly and epigenetic stability of centromeric chromatin (Ravi *et al.*, 2010; Fachinetti *et al.*, 2013; Folco *et al.*, 2015). Employing single-copy, targeted transgene insertion to replace endogenous CENP-A, we find that the N-tail of *C. elegans* CENP-A is essential for CENP-A loading, and we link this essential function to a direct interaction between the N-tail and the loading factor KNL-2/M18BP1. Interaction of the extended N-tail of *C. elegans* CENP-A to KNL-2/M18BP1 represents an evolutionary variation to HJURP/Scm3-mediated targeting of CENP-A to centromeres.

RESULTS

The *C. elegans* CENP-A N-tail has a predicted structured region that is essential for viability

The *C. elegans* CENP-A N-tail is unusually long at 189 amino acids and, based on computational analysis (performed using PSIPRED; http://bioinf.cs.ucl.ac.uk/psipred/), is predicted to have α-helical character in the first 100 amino acids (Figure 1A). The prediction of a structured region in the N-tail is unexpected as the CENP-A tail is often short (e.g., in fission yeast or humans, where it is 20 and 39 aa, respectively) and, even in other species with an extended CENP-A N-tail, such as *Drosophila melanogaster* (123 aa) or *S. cerevisiae* (130 aa), is not predicted to have any secondary structure (Figure 1A).

To test the functional significance of the predicted structured region of the *C. elegans* CENP-A N-tail, we developed a transgene-based system to replace endogenous CENP-A (named HCP-3 and referred to here as CENP-A$^{HCP\text{-}3}$) in *C. elegans* with engineered N-tail mutants. In brief, the nucleotide sequence of the *CENP-A$^{hcp\text{-}3}$* coding region was altered to maintain the native amino acid sequence while enabling selective RNAi-mediated depletion of endogenous CENP-A$^{HCP\text{-}3}$; in addition, an N-terminal GFP tag was added to monitor localization (Supplemental Figure S1A). The wild-type (WT), as well as two mutant transgenes (Δ109, which removes the predicted structured region, and Δ184, which removes the majority of the N-tail), were inserted in single copy at a fixed genomic location harboring a Mos transposon insertion (Figure 1B and Supplemental Figure S1A). The conditions we employ for RNAi penetrantly and selectively deplete the endogenous protein loaded into oocytes (Oegema and Hyman, 2006); in conjunction with RNAi-resistant transgenes, this approach enables replacing any targeted protein with a transgene-encoded version in the one-cell embryo. The reencoded *gfp::CENP-A$^{hcp\text{-}3}$* transgene rescued embryonic lethality observed following depletion of endogenous CENP-A$^{HCP\text{-}3}$ by RNAi as well as the lethality of a deletion mutant (*hcp-3(ok1892)*, referred to as *CENP-A$^{hcp\text{-}3}\Delta$*; Figure 1C and Supplemental Figure S1B). By contrast, deletion of the predicted structured region (Δ109) and of the majority of the N-tail (Δ184) resulted in fully penetrant embryonic lethality (Figure 1C). Immunoblotting with an antibody raised to the unstructured linker (amino acids 105–183 of the N-tail) indicated that the Δ109 mutant was expressed similarly to endogenous CENP-A$^{HCP\text{-}3}$ (Figure 1D); thus, the observed lethality is not because the Δ109 N-tail mutant is not expressed. We conclude that the predicted structured region of the N-tail of CENP-A is essential for viability of *C. elegans* embryos.

The CENP-A$^{HCP\text{-}3}$ N-tail deletion mutant exhibits a kinetochore-null phenotype in one-cell embryos

We next assessed the phenotype observed when endogenous CENP-A$^{HCP\text{-}3}$ was replaced by the Δ109 N-tail mutant. We crossed an mCherry::H2b marker into strains harboring single-copy transgenes expressing WT or Δ109 GFP::CENP-A$^{HCP\text{-}3}$, depleted endogenous CENP-A$^{HCP\text{-}3}$ by RNAi, and imaged one-cell embryos. As a

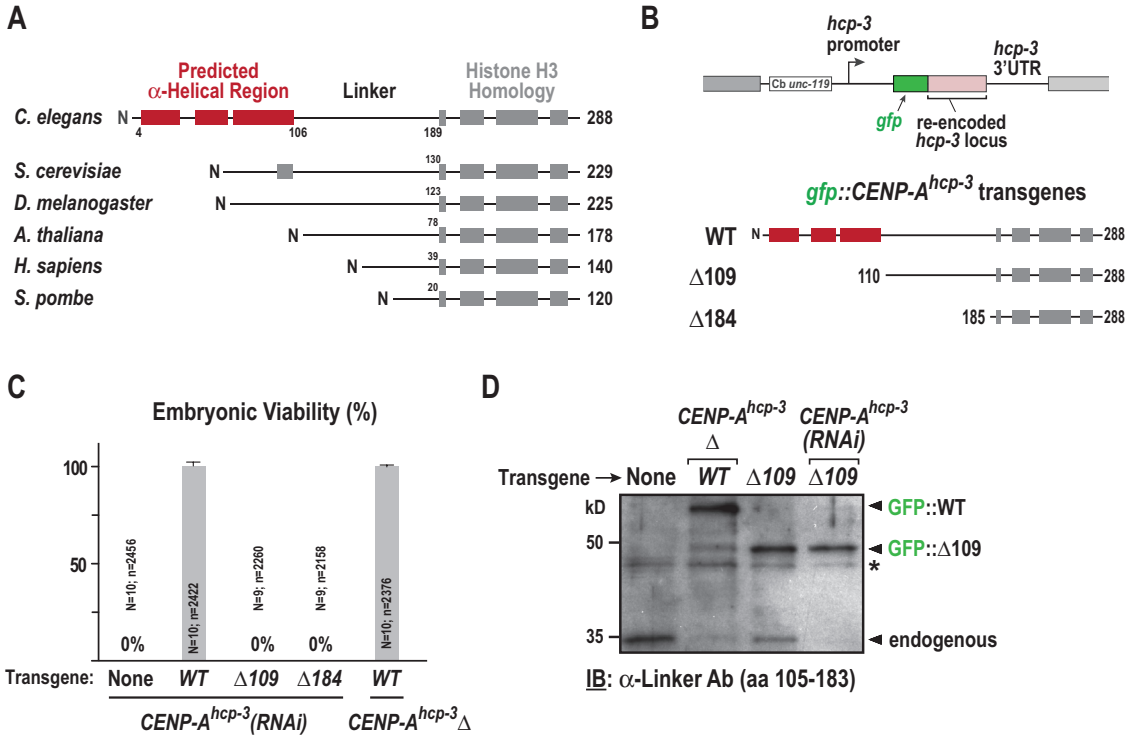

FIGURE 1: The extended N-tail of *C. elegans* CENP-A^{HCP-3} contains a predicted structured region that is essential for viability. (A) Secondary structure predictions of CENP-A from different model organism species. Secondary structure predictions were generated using PsiPred. Predicted α-helical segments are indicated as boxes. The histone fold domain (HFD) is marked in gray. (B) Schematic of RNAi-resistant *gfp::CENP-A^{hcp-3}* single-copy transgene insertions on chromosome II. The three variants of CENP-A^{HCP-3} expressed from single-copy transgene insertions are indicated below. (C) Embryo viability analysis for the indicated conditions. *N* refers to the number of worms and *n* to the total number of embryos scored. Error bars are the SEM. (D) Anti-CENP-A^{HCP-3} immunoblot performed using an antibody raised to the linker region (aa 105–183) showing expression levels of WT GFP-CENP-A^{HCP-3} and the Δ109 N-tail truncation mutant in the presence and absence of endogenous CENP-A^{HCP-3} (*Δ* indicates homozygous *CENP-A^{hcp-3}* deletion mutant; *(RNAi)* indicates *CENP-A^{hcp-3}(RNAi)*). Asterisk (*) marks a background band that serves as a loading control.

control, we also depleted CENP-A^{HCP-3} in the absence of any transgene. Depletion of CENP-A resulted in the characteristic kinetochore-null phenotype, with two clusters of chromatin—one from each pronucleus—instead of a metaphase plate, and a failure of segregation (Figure 2A; Oegema *et al.*, 2001; Desai *et al.*, 2003). This severe phenotype was fully rescued by transgene-encoded RNAi-resistant WT GFP::CENP-A^{HCP-3}. By contrast, the observed phenotype for the Δ109 N-tail mutant was similar to that of removal of CENP-A^{HCP-3} (Figure 2A). Thus, deletion of the first 109 amino acids of the N-tail of CENP-A^{HCP-3} results in a chromosome segregation phenotype that is equivalent to CENP-A^{HCP-3} removal in the *C. elegans* embryo.

The CENP-A^{HCP-3} N-tail deletion mutant does not accumulate on chromatin and fails to support kinetochore assembly

Stable incorporation of CENP-A into chromatin in yeast and humans involves a region of the histone fold, referred to as the CATD, which is specifically bound by the chaperone Scm3/HJURP (Black *et al.*, 2007; Cho and Harrison, 2011; Hu *et al.*, 2011). In these species, the N-tail is not essential for CENP-A centromere targeting, and alterations of the N-tail do not phenocopy loss of CENP-A (Chen *et al.*, 2000; Fachinetti *et al.*, 2013; Folco *et al.*, 2015). The similar phenotypes observed for CENP-A^{HCP-3} removal and for the Δ109 N-tail mutant of *C. elegans* CENP-A suggested that the Δ109 N-tail mutant, in contrast to the N-tail mutants in other species, may not accumulate on centromeric chromatin. To test this idea, we imaged WT and Δ109 GFP::CENP-A^{HCP-3} in a strain coexpressing mCherry::H2b, and quantified the GFP signal on metaphase chromosomes. In the presence of endogenous CENP-A^{HCP-3}, both WT and Δ109 GFP::CENP-A^{HCP-3} localized to the diffuse kinetochores on the poleward faces of the holocentric mitotic chromosomes (Figure 2B) and quantification of fluorescence intensity indicated equivalent localization of both (Figure 2C). However, in the absence of endogenous CENP-A^{HCP-3}, localization of Δ109 GFP::CENP-A^{HCP-3} was greatly reduced relative to WT GFP::CENP-A^{HCP-3} (Figure 2, B and C). Thus, Δ109 GFP::CENP-A^{HCP-3} fails to localize to chromatin on its own.

The absence of the Δ109 CENP-A^{HCP-3} mutant in chromatin should result in a kinetochore assembly defect. To confirm that this was indeed the case, we analyzed the localization of an RNAi-resistant mCherry-fusion of KNL-1, an outer kinetochore scaffold protein (Desai *et al.*, 2003; Espeut *et al.*, 2012). We introduced the transgene expressing this fusion into the strain expressing either WT or Δ109 GFP::CENP-A^{HCP-3}, depleted endogenous KNL-1 and CENP-A^{HCP-3}, and imaged and quantified the KNL-1::mCherry signal. This analysis revealed that loss of KNL-1::mCherry localization in the Δ109 GFP::CENP-A^{HCP-3} mutant was analogous to the CENP-A^{HCP-3} depletion (Figure 2, D and E). Thus, the Δ109 CENP-A^{HCP-3} mutant fails to support kinetochore assembly.

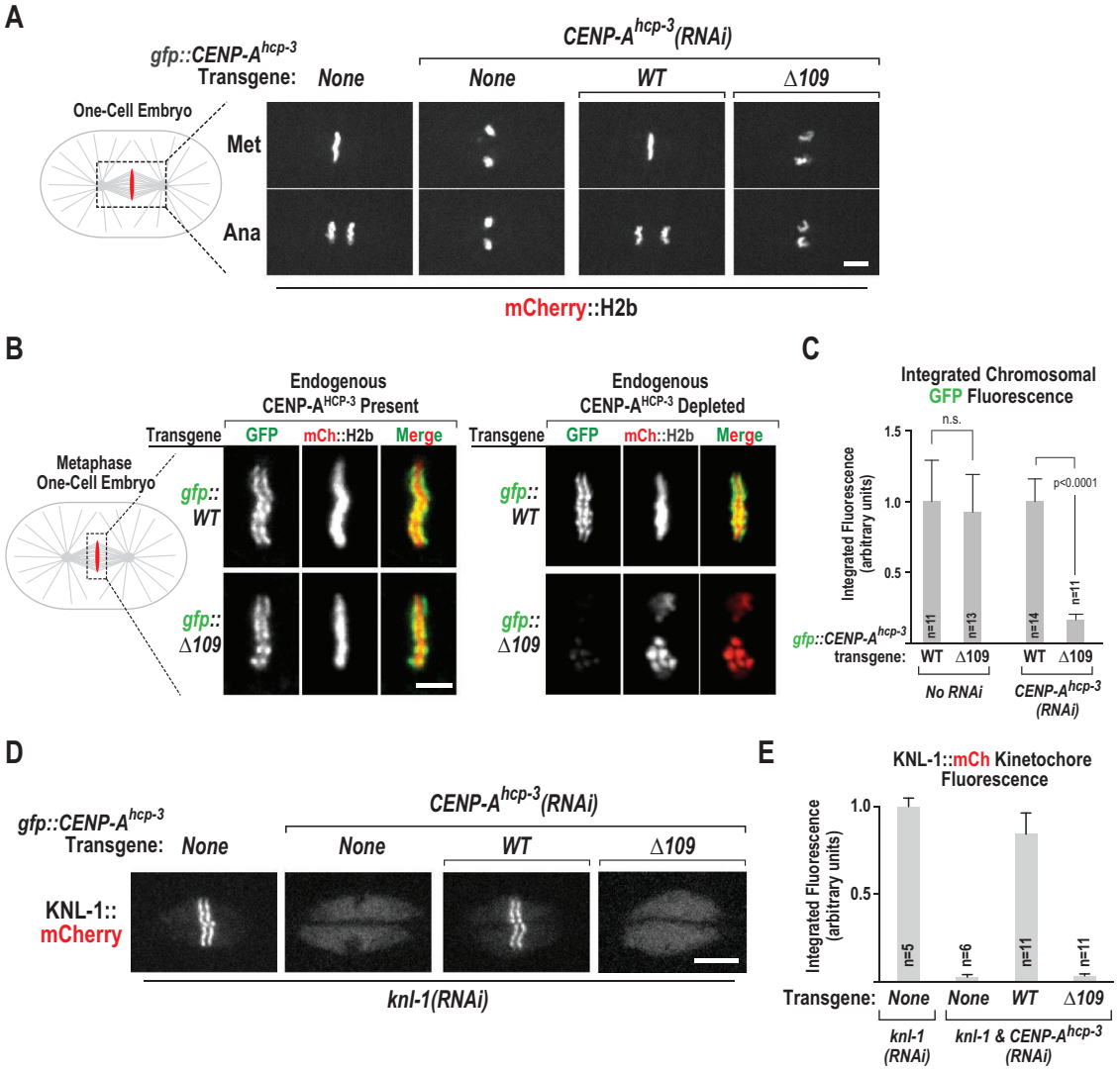

FIGURE 2: Deletion of the predicted α-helical region of the CENP-A^{HCP-3} N-tail results in a kinetochore-null phenotype and failure to accumulate on mitotic chromatin. (A) mCherry::H2b images from time-lapse sequences for the indicated conditions in metaphase- and anaphase-stage one-cell embryos. Similar results were obtained in at least 10 embryos per condition. Scale bar, 5 μm. (B) Images of WT and Δ109 GFP::CENP- $^{HCP-3\Delta}$ in metaphase-stage embryos expressing mCherry-H2b in the presence (left set of panels) or absence (right set of panels) of endogenous CENP-A^{HCP-3}. Scale bar, 2.5 μm. (C) Quantification of integrated chromosomal GFP intensity in metaphase-stage embryos for the indicated conditions. *t* tests were used to assess if indicated pairwise comparisons were significantly different. Error bars are the SD. (D) Images of KNL-1::mCherry, expressed from an integrated single-copy RNAi-resistant transgene, in metaphase-stage one-cell embryos for the indicated conditions; note that endogenous KNL-1 was depleted in all cases. Scale bar, 5 μm. (E) Quantification of integrated KNL-1::mCherry kinetochore intensity in metaphase-stage embryos for the indicated conditions. Error bars are the SD.

The failure of the CENP-A^{HCP-3} N-tail deletion mutant to accumulate on chromatin is not due to a kinetochore assembly defect

CENP-A^{HCP-3} is essential for kinetochore assembly (Oegema *et al.*, 2001). However, preventing kinetochore assembly by depleting CENP-C^{HCP-4} or KNL-1, both of which result in a similar kinetochore-null phenotype as CENP-A^{HCP-3} depletion (Oegema *et al.*, 2001; Desai *et al.*, 2003), does not affect GFP::CENP-A^{HCP-3} chromatin accumulation (Figures 2B and 3, A and B). Thus, the absence of Δ109 CENP-A^{HCP-3} on chromatin cannot be a secondary consequence of defective kinetochore assembly.

CENP-A^{HCP-3} depletion, in addition to the kinetochore-null phenotype, also leads to defects in condensation of the holocentric *C. elegans* chromosomes (Maddox *et al.*, 2006, 2007). By contrast, preventing kinetochore formation by depletion of CENP-C^{HCP-4} does not result in a similarly severe condensation defect (Maddox *et al.*, 2006). We therefore compared chromosome condensation in CENP-A^{HCP-3} and CENP-C^{HCP-4} depletion to that in the Δ109 CENP-A^{HCP-3} tail mutant (Figure 3C); we additionally assessed if WT GFP::CENP-A^{HCP-3} rescued the condensation defect observed in the CENP-A^{HCP-3} depletion (Figure 3D). This analysis focused on sperm pronuclei as they are formed before injection of the dsRNA employed to deplete endogenous CENP-A^{HCP-3} and are therefore free of potential meiotic defects (Maddox *et al.*, 2006). Chromosome condensation in the Δ109 CENP-A^{HCP-3} mutant resembled that resulting from CENP-A^{HCP-3} depletion and not CENP-C^{HCP-4} depletion

(Figure 3C); in addition, transgene-encoded WT CENP-A^{HCP-3} rescued the condensation defect of CENP-A^{HCP-3} depletion (Figure 3D). These results provide additional support for the conclusion that the Δ109 mutant is compromised for its loading onto chromatin. When considered in light of prior work showing that CENP-A^{HCP-3} is loaded de novo on chromatin in one-cell *C. elegans* embryos (Gassmann *et al.*, 2012), the above results indicate that the absence of Δ109 CENP-A^{HCP-3} on chromatin is due to a defect in its loading after fertilization.

The predicted α-helical region of the CENP-A tail interacts with the CENP-A loading factor KNL-2

The above results implicate the predicted structured region of the N-tail of *C. elegans* CENP-A^{HCP-3} in its loading on chromatin. In species with Scm3/HJURP, a key step in the loading reaction is the interaction of the Scm3/HJURP-CENP-A complex with the Mis18 complex, which includes the Myb domain–containing protein KNL-2 (also known as M18BP1 or Mis18BP1, based on its association with Mis18α/β in human cells; Fujita *et al.*, 2007; Maddox *et al.*, 2007; Wang *et al.*, 2014; French *et al.*, 2017; Pan *et al.*, 2019; to date, a Mis18α/β homologue has not been identified in *C. elegans*). In addition, Scm3/HJURP functions as a chaperone for assembly of CENP-A nucleosomes (Dunleavy *et al.*, 2009; Foltz *et al.*, 2009; Pidoux *et al.*, 2009; Williams *et al.*, 2009; Shuaib *et al.*, 2010).

To determine how the N-tail of CENP-A^{HCP-3} contributes to its loading, we tested if it interacts with KNL-2. KNL-2 family proteins are characterized by a conserved Myb-like DNA-binding domain and a predicted folded N-terminal domain referred to as the SANTA domain (Figure 4A; Zhang *et al.*, 2006; Maddox *et al.*, 2007); in addition, they possess an acidic/aromatic tail at the C-terminus (Supplemental Figure S2A). Using yeast two-hybrid analysis, we observed a robust interaction between a segment of the middle region of KNL-2 (residues 267–470; predicted to be unstructured) and the predicted α-helical region of the N-tail of CENP-A^{HCP-3} (Figure 4B); an interaction between KNL-2 and CENP-A^{HCP-3} was also reported in a large-scale two-hybrid screen of proteins essential for *C. elegans* embryogenesis (Boxem *et al.*, 2008). This interaction was not observed with full-length KNL-2 but, as no interaction has been observed with this fusion, this may be a false negative due to the full-length protein not being properly expressed/folded in yeast; a similar caveat also applies to the SANTA domain- and C-terminal KNL-2 fragments that did not show any interaction. Importantly, an interaction between similar regions of CENP-A^{HCP-3} and KNL-2 was also observed for the *Caenorhabditis briggsae* proteins (Figure 4B), despite primary sequence divergence (23.7% identity/43.5% similarity for CENP-A^{HCP-3} N-tail and 42.9% identity/55.1% similarity for KNL-2 middle region; Supplemental Figure S2B). The interaction was species specific, as the *C. briggsae* CENP-A^{HCP-3} N-tail did not interact with *C. elegans* KNL-2 middle region and vice versa (Figure 4B).

To confirm the two-hybrid interaction, we performed pull-down assays with a purified MBP-His6 fusion of the CENP-A^{HCP-3} N-tail immobilized on nickel agarose and in vitro–translated MBP-KNL-2 fragments. We first screened a series of overlapping fragments of KNL-2 and found that, consistent with the yeast two-hybrid results, a fragment containing residues 301–500 interacted with the N-tail (Figure 4C); we note that this KNL-2 fragment exhibited variable background interaction with the MBP-only control (Figure 4E); however, the interaction with CENP-A^{HCP-3} N-tail MBP fusion was consistently above background. We next analyzed a series of truncated fragments in this region and found that a central region of 50 amino acids (376–425) was essential for the interaction (Figure 4, D and E). However, this 50–amino acid region on its own did not interact with the CENP-A^{HCP-3} N-tail (Figure 4E), suggesting that residues on either side are important for the observed interaction. We conclude that the predicted α-helical region of the N-tail of CENP-A^{HCP-3} that is important for chromatin loading in vivo interacts directly with the CENP-A^{HCP-3} loading factor KNL-2 in vitro and that this interaction is conserved in a related nematode species with a significantly diverged N-tail sequence.

DISCUSSION

Here, we investigated how CENP-A chromatin is assembled in the absence of a HJURP/Scm3 family protein in *C. elegans*. We found that the unusually long N-tail of *C. elegans* CENP-A, which contains a predicted α-helical region, is required for CENP-A loading onto chromatin. By contrast, the divergent N-tails of CENP-A family members have been proposed to contribute to kinetochore assembly and to epigenetic stability of centromeric chromatin (Ravi *et al.*, 2010; Fachinetti *et al.*, 2013; Folco *et al.*, 2015), but have not been implicated in assembly of CENP-A chromatin. By comparing deletion of the predicted structured region of the CENP-A N-tail to two other perturbations that prevent kinetochore assembly, we show that the absence of N-tail-mutant CENP-A^{HCP-3} on chromatin is due to a failure in loading and not a consequence of defective kinetochore assembly. In addition, as the N-tail-mutant CENP-A^{HCP-3} localizes normally in the presence of endogenous CENP-A^{HCP-3}, the absence of localization cannot be attributed to misfolding or inability to interact with histone H4. Thus, the N-tail effectively acts as an intramolecular-targeting signal, analogous to the CATD in HJURP/Scm3-containing species.

CENP-A^{HCP-3} is loaded de novo in the one-cell *C. elegans* embryo (Gassmann *et al.*, 2012). Thus, whether the N-tail-KNL-2 interaction reported here continues to be required to load CENP-A^{HCP-3} after de novo loading in the first embryonic division is an important question. A recent study reported that embryos homozygous mutant for N-tail deleted CENP-A^{HCP-3}, derived from a heterozygous parent and thus having maternally loaded full-length CENP-A^{HCP-3}, developed into adults; by contrast, embryos homozygous null mutant for CENP-A^{HCP-3} derived from a heterozygous parent did not (Prosée *et al.*, 2020). This observation indicates that the N-tail-deleted CENP-A^{HCP-3} supports development following depletion of maternally loaded full-length CENP-A^{HCP-3}, suggesting that the N-tail may not be essential for loading later in embryogenesis. However, an alternative possibility is raised by the observation that N-tail deleted CENP-A^{HCP-3} localizes to centromeres in the presence of full-length CENP-A^{HCP-3}, likely due to the presence of 2 CENP-As in octameric centromeric nucleosomes. Thus, N-tail-deleted CENP-A^{HCP-3} may stabilize/enhance the functionality of maternally loaded full-length CENP-A^{HCP-3}, and thereby lead to a less severe developmental phenotype. Development of acute means of removing maternally loaded CENP-A^{HCP-3} after the initial de novo loading in the early embryo will be necessary to address whether the N-tail is required for loading throughout embryogenesis or whether its role in loading is restricted to early embryonic divisions.

HJURP/Scm3 has two roles: one is to act as a chaperone promoting assembly of CENP-A nucleosomes, and the second is to target this assembly reaction to centromeric chromatin through an interaction with centromere recognition factors (Ndc10 in budding yeast, Mis18 in fission yeast, KNL-2 in *C. elegans* and plants, and Mis18 complex in vertebrates). Through two-hybrid and in vitro biochemical assays, we provide evidence that the *C. elegans* CENP-A N-tail possesses the latter activity; it interacts directly with the middle region of KNL-2 and this interaction is preserved in a species-specific manner in *C. briggsae*, despite significant primary sequence divergence (especially in the

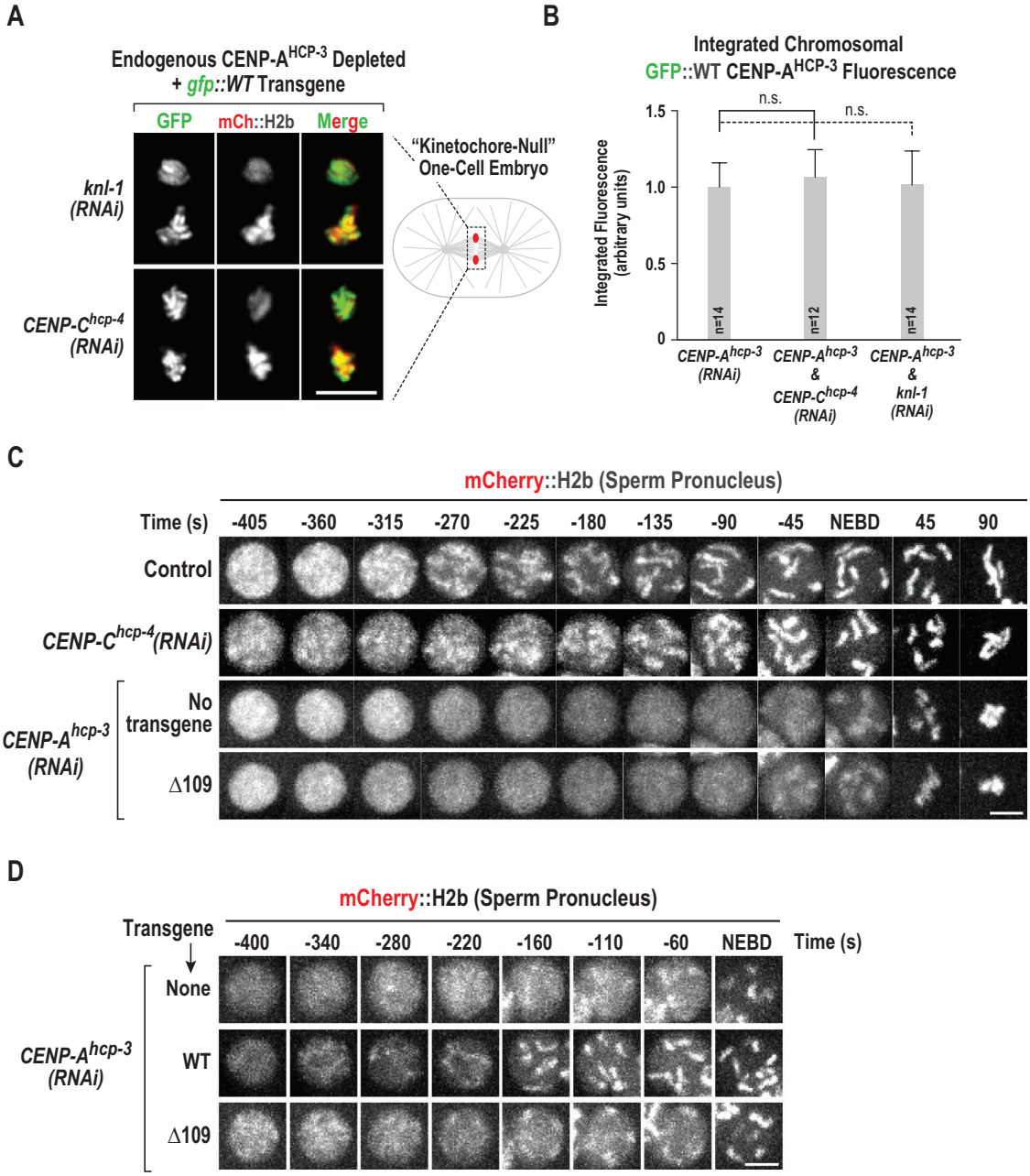

FIGURE 3: Inability of Δ109 CENP-A^{HCP-3} to accumulate on chromatin is not due to failure of kinetochore assembly. (A) Images of WT GFP::CENP-A^{HCP-3} in metaphase-stage embryos also expressing mCherry::H2b that were depleted of endogenous CENP-A^{HCP-3} and KNL-1 (top) or CENP-C^{HCP-4} (bottom). Scale bar, 5 μm. (B) Quantification of integrated chromosomal WT GFP::CENP-A $^{HCP-3}$ intensity in metaphase-stage embryos for the indicated conditions. The *CENP-A^{hcp-3}(RNAi)* alone value is the same as in Figure 2C. Error bars are the SD. *t* tests were employed to assess statistical significance of indicated pairwise comparisons. (C, D) Images of mCherry::H2b in sperm pronuclei from time-lapse sequences for the indicated conditions. Times are in seconds after nuclear envelope breakdown (NEBD). Similar results were observed in at least 10 embryos filmed per condition. Scale bar, 5 μm.

N-tail sequence). A recent study independently described a CENP-A^{HCP-3} N-tail–KNL-2 interaction that is consistent with what we report here (Prosée *et al.*, 2020). To date, we have been unable to selectively mutate this interaction and assess the consequences in vivo; this will be important to pursue in the future. An obvious question emerging from our results is whether the N-tail of CENP-A^{HCP-3} also exhibits chaperone activity, analogous to HJURP/Scm3. In preliminary work, we have not observed an interaction between the N-tail and the histone fold of CENP-A^{HCP-3} in two-hybrid and in vitro binding assays, which would argue against the presence of chaperone activity. However, significantly more effort needs to be placed on reconstitutions with purified components to address whether these negative results are indeed due to an absence of chaperone activity. RNAi experiments have implicated the *C. elegans* orthologue of the histone-binding WD40 domain chaperone RbAp46/48, LIN-53, in CENP-A^{HCP-3} chromatin assembly (Lee *et al.*, 2016), suggesting that it may work together with the CENP-A^{HCP-3} N-tail–KNL-2 interaction described here to assemble centromeric chromatin.

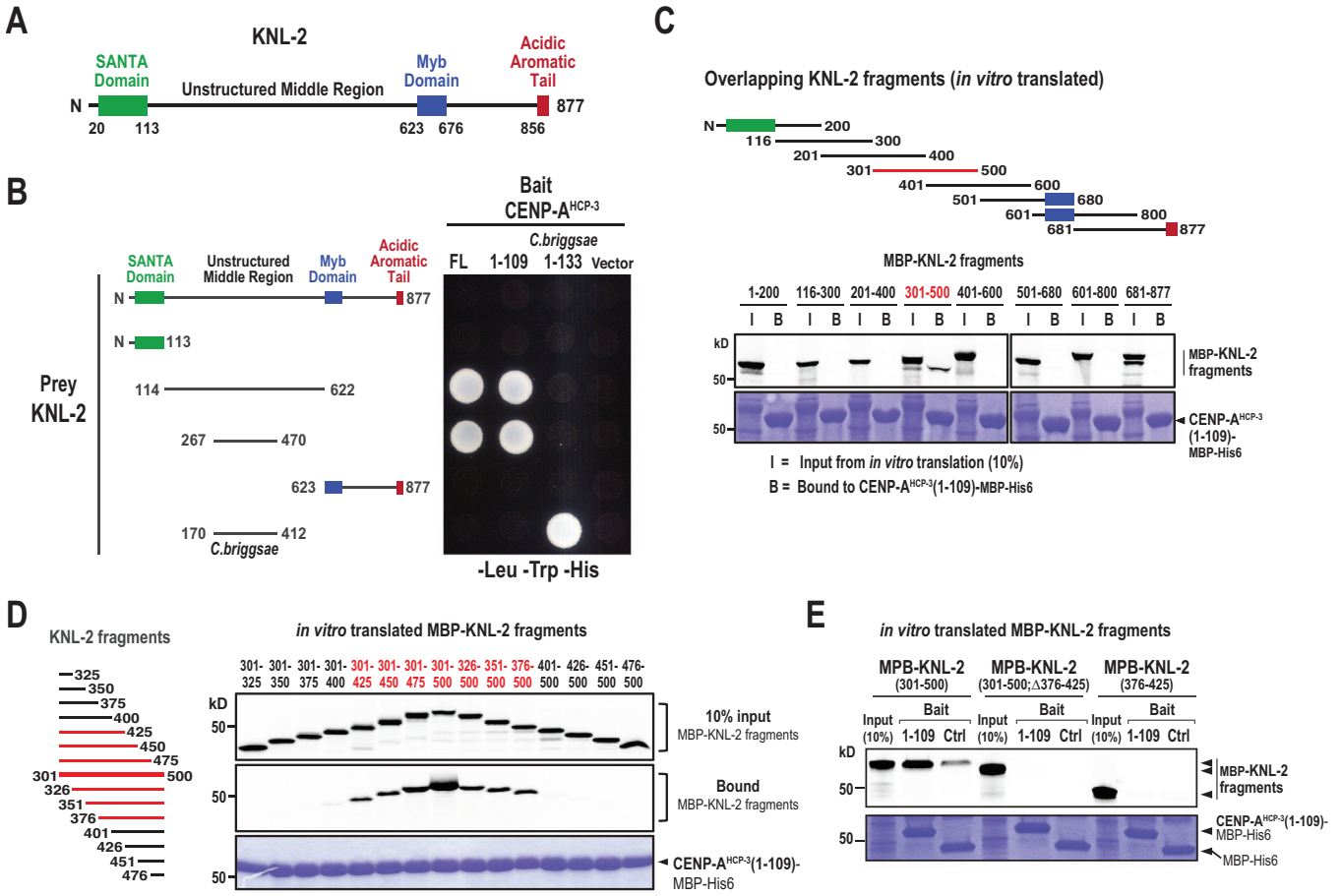

FIGURE 4: The N-tail of CENP-A^{HCP-3} interacts with an unstructured middle region of KNL-2. (A) Domain structure of KNL-2. The presence of the SANTA domain (PF09133) and the Myb domain (also known as the SANT domain; PF00249) is conserved among the KNL-2/M18BP1 protein family. No secondary structure elements are predicted in the middle region of KNL-2. (B) Yeast two-hybrid analysis of CENP-A^{HCP-3} N-tail and KNL-2. The bait CENP-A^{HCP-3} N-tail fusions are listed on top and the prey KNL-2 fusions are listed on the left. (C–E) Biochemical analysis of the CENP-A^{HCP-3}-KNL-2 interaction. Nickel-immobilized recombinant CENP-A^{HCP-3}(1–109)-MBP-His$_6$ was used to pull down indicated reticulocyte lysate-expressed S^{35}-labeled MBP-KNL-2 fragments. In C, S^{35}-autoradiogram (top) shows Input (I) and bead-bound (B) KNL-2 fragments; Coomassie staining (bottom) shows input lysate and CENP-A^{HCP-3}(1–109)-MBP-His$_6$ bait. In D, fragments of the 301–500 amino acid region of KNL-2 tested for binding to CENP-A^{HCP-3}(1–109) are schematized on the left. S^{35}-autoradiogram (top) shows reticulocyte lysate-expressed MBP-KNL-2 fragments; S^{35}-autoradiogram (middle) shows bound KNL-2 fragments; Coomassie staining (bottom) shows CENP-A^{HCP-3} N-tail bait. In E, indicated KNL-2 fragments were tested for binding to control (MBP-His$_6$) and CENP-A^{HCP-3}(1–109)-MBP-His$_6$ baits. S^{35}-autoradiogram (top) shows input and bound fragments; Coomassie staining (bottom) shows input lysates and baits.

In conclusion, we provide evidence for an evolutionary variation on CENP-A chromatin assembly in which the N-tail of CENP-A has acquired part of the function of the specialized chaperone/targeting factor HJURP/Scm3 and become essential for loading into chromatin. This represents a distinct solution from *Drosophila*, which also lacks HJURP/Scm3 but appears to have convergently evolved an HJURP/Scm3-like chaperone called Cal1 (Erhardt *et al.*, 2008; Phansalkar *et al.*, 2012; Chen *et al.*, 2014; Medina-Pritchard *et al.*, 2020). Understanding how different species build CENP-A chromatin at restricted genomic locations should provide insight into the general principles by which the epigenetic state of centromeric chromatin is defined and propagated.

MATERIALS AND METHODS

Request a protocol through *Bio-protocol*.

C. *elegans* strains

C. elegans strains (genotypes in Supplemental Table S1) were maintained at 20°C (Edgley *et al.*, 2006). Engineered GFP::CENP-A^{HCP-3} transgenes were cloned into pCFJ151 and injected into strain EG4322. The KNL-1::mCherry transgene was cloned into pCFJ178 and injected into EG6700 (Frokjaer-Jensen *et al.*, 2008). The amplified *hcp-3* genomic locus was flanked on the 5′ end by 5′-GACGACGCTCCGAATCATTTGGGAG-3′ and on the 3′ end by 5′-CTATTTGTCAAATAATAAAGATTCATTACTTGTAAATGAGAACATTTTATTTAA-3′. For the GFP:: CENP-A^{HCP-3} transgenes the GFP sequence was inserted following the start codon and preceded by a GGRAGSGGRAGSGGRAGS linker. All exons were reencoded in *CENP-A^{hcp-3}* to allow RNAi-mediated depletion of endogenous CENP-A without affecting the introduced transgene. Single-copy insertion was confirmed by PCR. Transgenic strains were crossed into various marker or deletion strains using standard genetic procedures.

RNA-mediated interference (RNAi)

Double-stranded RNAs were generated using oligos (Supplemental Table S2) to amplify regions from N2 genomic DNA or cDNA. PCR reactions were used as templates for in vitro RNA production (Ambion), and the RNA was purified using a MegaClear kit (Ambion). Eluted RNA from the T3 and T7 reactions were mixed together, combined with 3× soaking buffer (32.7 mM Na_2HPO_4, 16.5 mM KH_2PO_4, 6.3 mM KCl, 14.1 mM NH_4Cl), and annealed (68°C for 10 min, 37°C for 30 min). dsRNA was injected into L3/L4 hermaphrodite worms 38–42 h before imaging. For double depletions dsRNAs were mixed in equal amounts (≥1–3 mg/ml for each RNA).

Immunoblotting

For immunoblotting a mixed population of worms growing at 20°C on an NGM+OP50 agar plate were collected with M9+0.1% Triton X-100, pelleted, and washed. Worms were vortexed in a mix of 100 µl M9+0.1% Triton X-100, 50 µl 4× sample buffer, and 100 µl glass beads and boiled, then vortexed and boiled again. Samples were run on an SDS–PAGE gel, transferred to a polyvinylidene fluoride membrane, probed with 1 µg/ml affinity-purified anti-CENP-$A^{HCP\text{-}3}$ (rabbit; antigen was CENP-$A^{HCP\text{-}3}$[105–183]::6xHis) and detected using an horseradish peroxidase–conjugated secondary antibody (rabbit or mouse; GE Healthcare). For antibody production CENP-$A^{HCP\text{-}3}$(105–183)::6xHis was expressed in *Escherichia coli*, purified, and injected into rabbits (Covance). Serum was affinity purified on a HiTrap NHS column to which CENP-$A^{HCP\text{-}3}$(105–183)::6xHis was covalently coupled.

Yeast two-hybrid screens

Yeast two-hybrid analysis was performed according to the manufacturer guidelines (Matchmaker; Clontech Laboratories). Genes of interest were cloned from WT (N2) *C. elegans* or *C. briggsae* cDNA.

Imaging and quantification

For live imaging of one-cell embryos, gravid hermaphrodite adult worms were dissected into M9 buffer, embryos were manually transferred to 2% agarose pads, and overlaid with a coverslip. For all experiments, except the one shown in Figure 3D, a 5 × 2 µm z-series was collected every 10–15 s using an inverted Zeiss Axio Observer Z1 system with a Yokogawa spinning-disk confocal head (CSU-X1), a 63×, 1.4 NA Plan Apochromat objective, and a QuantEM 512SC EMCCD camera (Photometrics). For the experiment shown in Figure 3D, 6 × 2 µm z-series were acquired every 10 s using an Andor Revolution XD Confocal System (Andor Technology), with a CSU-10 spinning-disk confocal scanner unit (Yokogawa) mounted on a TE2000-E inverted microscope (Nikon), 60×, 1.4 NA Plan Apochromat lenses, and a back-thinned EMCCD camera (iXon, Andor Technology). Environmental temperature during image acquisition was 19°–20°C.

All images and movies were processed, scaled, and analyzed using ImageJ (Fiji) and Photoshop (Adobe). Quantification of CENP-$A^{HCP\text{-}3}$ and KNL-1 kinetochore localization during metaphase of one-cell embryos was performed on maximum intensity projections. A rectangle was drawn around the fluorescence signal and average pixel intensity was measured. The rectangle was expanded on all sides and the difference in integrated intensity between the expanded rectangle and the original rectangle was used to define the background intensity per pixel. Integrated fluorescence was then calculated for the original rectangle after background subtraction (Moyle *et al.*, 2014).

Protein purification

CENP-$A^{HCP\text{-}3}$(1–109)-MBP-6xHis was cloned into pET21a. HCP-3(1–109)-MBP-6xHis and MBP::6xHis were expressed in BL21(DE3). *E. coli* cultures were grown to OD_{600} 0.6–0.8 and induced with 0.1 mM IPTG (isopropyl-β-D-thiogalactoside) for 6 h at 20°C. Induced BL21(DE3) cells were lysed in lysis buffer (20 mM Tris, pH 7.5, 300 mM NaCl, 20 mM imidazole, 8 mM β-mercaptoethanol [BME]) and clarified at 40,000 × *g* for 45 min at 4°C. Ni-NTA agarose (Qiagen) was incubated with clarified lysates for 45 min, washed with wash buffer (20 mM Tris, pH 7.5, 300 mM NaCl, 50 mM imidazole, 8 mM BME), and eluted with 20 mM Tris, pH 7.5, 300 mM NaCl, 300 mM imidazole, 8 mM BME. The eluted protein was fractionated using a Superose10 gel filtration column (GE Healthcare). Protein concentrations were determined using a NanoDrop 1000 spectrophotometer (Thermo Scientific).

In vitro translation and binding assay

KNL-2-MBP fragments were $^{[35]}S$ labeled using a TnT Quick Coupled Transcription/Translation System (Promega). In vitro translation lysate (10 µl) was incubated for 1 h at 4°C with 50 µg CENP-$A^{HCP\text{-}3}$(1–109)-MBP-His (in 20 mM Tris, pH7.5, 300 mM NaCl, 0.05% NP40, 10 mM imidazole) in a final volume of 50 µl, mixed with 25 µl of a 1:1 nickel agarose slurry equilibrated with the binding buffer for an additional hour at 4°C. Beads were washed three times with binding buffer, eluted using sample buffer, and the elution analyzed by SDS–PAGE and autoradiography.

ACKNOWLEDGMENTS

We thank the Caenorhabditis Genetics Center for providing the *CENP-A$^{hcp\text{-}3}$* null mutant. This work was supported by a National Institutes of Health grant (Grant no. GM-074215) to A.D., a German Research Foundation grant (Grant no. GR 3859/1-1) to C.D.G., a National Science Foundation Graduate Research Fellowship to J.H., and an EMBO Fellowship (ALTF 251-2012) to A.G-G. A.D., K.O., and A.K.S. received salary and other support from Ludwig Cancer Research.

REFERENCES

Allshire RC, Karpen GH (2008). Epigenetic regulation of centromeric chromatin: old dogs, new tricks? Nat Rev Genet 9, 923–937.

Barnhart MC, Kuich PH, Stellfox ME, Ward JA, Bassett EA, Black BE, Foltz DR (2011). HJURP is a CENP-A chromatin assembly factor sufficient to form a functional de novo kinetochore. J Cell Biol 194, 229–243.

Black BE, Foltz DR, Chakravarthy S, Luger K, Woods VL Jr, Cleveland DW (2004). Structural determinants for generating centromeric chromatin. Nature 430, 578–582.

Black BE, Jansen LE, Maddox PS, Foltz DR, Desai AB, Shah JV, Cleveland DW (2007). Centromere identity maintained by nucleosomes assembled with histone H3 containing the CENP-A targeting domain. Mol Cell 25, 309–322.

Boxem M, Maliga Z, Klitgord N, Li N, Lemmens I, Mana M, de Lichtervelde L, Mul JD, van de Peut D, Devos M, *et al.* (2008). A protein domain-based interactome network for *C.elegans* early embryogenesis. Cell 134, 534–545.

Chen Y, Baker RE, Keith KC, Harris K, Stoler S, Fitzgerald-Hayes M (2000). The N terminus of the centromere H3-like protein Cse4p performs an essential function distinct from that of the histone fold domain. Mol Cell Biol 20, 7037–7048.

Chen CC, Dechassa ML, Bettini E, Ledoux MB, Belisario C, Heun P, Luger K, Mellone BG (2014). CAL1 is the *Drosophila* CENP-A assembly factor. J Cell Biol 204, 313–329.

Cho US, Harrison SC (2011). Recognition of the centromere-specific histone Cse4 by the chaperone Scm3. Proc Natl Acad Sci USA 108, 9367–9371.

Desai A, Rybina S, Muller-Reichert T, Shevchenko A, Shevchenko A, Hyman A, Oegema K (2003). KNL-1 directs assembly of the microtubule-binding interface of the kinetochore in *C.elegans*. Genes Dev 17, 2421–2435.

Dunleavy EM, Roche D, Tagami H, Lacoste N, Ray-Gallet D, Nakamura Y, Daigo Y, Nakatani Y, Almouzni-Pettinotti G (2009). HJURP is a cell-cycle-dependent maintenance and deposition factor of CENP-A at centromeres. Cell 137, 485–497.

Edgley ML, Baillie DL, Riddle DL, Rose AM (2006). Genetic balancers. WormBook 1–32.
Erhardt S, Mellone BG, Betts CM, Zhang W, Karpen GH, Straight AF (2008). Genome-wide analysis reveals a cell cycle–dependent mechanism controlling centromere propagation. J Cell Biol 183, 805–818.
Espeut J, Cheerambathur DK, Krenning L, Oegema K, Desai A (2012). Microtubule binding by KNL-1 contributes to spindle checkpoint silencing at the kinetochore. J Cell Biol 196, 469–482.
Fachinetti D, Folco HD, Nechemia-Arbely Y, Valente LP, Nguyen K, Wong AJ, Zhu Q, Holland AJ, Desai A, Jansen LE, Cleveland DW (2013). A two-step mechanism for epigenetic specification of centromere identity and function. Nat Cell Biol 15, 1056–1066.
Folco HD, Campbell CS, May KM, Espinoza CA, Oegema K, Hardwick KG, Grewal SIS, Desai A (2015). The CENP-A N-tail confers epigenetic stability to centromeres via the CENP-T branch of the CCAN in fission yeast. Curr Biol 25, 348–356.
Foltz DR, Jansen LE, Bailey AO, Yates JR 3rd, Bassett EA, Wood S, Black BE, Cleveland DW (2009). Centromere-specific assembly of CENP-A nucleosomes is mediated by HJURP. Cell 137, 472–484.
French BT, Straight AF (2019). CDK phosphorylation of *Xenopuslaevis* M18BP1 promotes its metaphase centromere localization. EMBO J 38, e100093.
French BT, Westhorpe FG, Limouse C, Straight AF (2017). *Xenopuslaevis* M18BP1 directly binds existing CENP-A nucleosomes to promote centromeric chromatin assembly. Dev Cell 42, 190–199.e110.
Frokjaer-Jensen C, Davis MW, Hopkins CE, Newman BJ, Thummel JM, Olesen SP, Grunnet M, Jorgensen EM (2008). Single-copy insertion of transgenes in *Caenorhabditiselegans*. Nat Genet 40, 1375–1383.
Fujita Y, Hayashi T, Kiyomitsu T, Toyoda Y, Kokubu A, Obuse C, Yanagida M (2007). Priming of centromere for CENP-A recruitment by human hMis18α, hMis18β, and M18BP1. Dev Cell 12, 17–30.
Gassmann R, Rechtsteiner A, Yuen KW, Muroyama A, Egelhofer T, Gaydos L, Barron F, Maddox P, Essex A, Monen J, *et al*. (2012). An inverse relationship to germline transcription defines centromeric chromatin in *C.elegans*. Nature 484, 534–537.
Hayashi T, Fujita Y, Iwasaki O, Adachi Y, Takahashi K, Yanagida M (2004). Mis16 and Mis18 are required for CENP-A loading and histone deacetylation at centromeres. Cell 118, 715–729.
Hori T, Shang WH, Hara M, Ariyoshi M, Arimura Y, Fujita R, Kurumizaka H, Fukagawa T (2017). Association of M18BP1/KNL2 with CENP-A nucleosome is essential for centromere formation in non-mammalian vertebrates. Dev Cell 42, 181–189 e183.
Hu H, Liu Y, Wang M, Fang J, Huang H, Yang N, Li Y, Wang J, Yao X, Shi Y, *et al*. (2011). Structure of a CENP-A-histone H4 heterodimer in complex with chaperone HJURP. Genes Dev 25, 901–906.
Jansen LE, Black BE, Foltz DR, Cleveland DW (2007). Propagation of centromeric chromatin requires exit from mitosis. J Cell Biol 176, 795–805.
Kato H, Jiang J, Zhou BR, Rozendaal M, Feng H, Ghirlando R, Xiao TS, Straight AF, Bai Y (2013). A conserved mechanism for centromeric nucleosome recognition by centromere protein CENP-C. Science 340, 1110–1113.
Kixmoeller K, Allu PK, Black BE (2020). The centromere comes into focus: from CENP-A nucleosomes to kinetochore connections with the spindle. Open Biol 10, 200051.
Lee BC, Lin Z, Yuen KW (2016). RbAp46/48(LIN-53) is required for holocentromere assembly in *Caenorhabditiselegans*. Cell Rep 14, 1819–1828.
Lermontova I, Kuhlmann M, Friedel S, Rutten T, Heckmann S, Sandmann M, Demidov D, Schubert V, Schubert I (2013). *Arabidopsis* kinetochore null2 is an upstream component for centromeric histone H3 variant cenH3 deposition at centromeres. Plant Cell 25, 3389–3404.
Maddox PS, Hyndman F, Monen J, Oegema K, Desai A (2007). Functional genomics identifies a Myb domain–containing protein family required for assembly of CENP-A chromatin. J Cell Biol 176, 757–763.
Maddox PS, Portier N, Desai A, Oegema K (2006). Molecular analysis of mitotic chromosome condensation using a quantitative time-resolved fluorescence microscopy assay. Proc Natl Acad Sci USA 103, 15097–15102.
McKinley KL, Cheeseman IM (2016). The molecular basis for centromere identity and function. Nat Rev Mol Cell Biol 17, 16–29.
Medina-Pritchard B, Lazou V, Zou J, Byron O, Abad MA, Rappsilber J, Heun P, Jeyaprakash AA (2020). Structural basis for centromere maintenance by *Drosophila* CENP-A chaperone CAL1. EMBO J 39, e103234.
Mellone BG, Grive KJ, Shteyn V, Bowers SR, Oderberg I, Karpen GH (2011). Assembly of *Drosophila* centromeric chromatin proteins during mitosis. PLoS Genet 7, e1002068.
Melters DP, Paliulis LV, Korf IF, Chan SW (2012). Holocentric chromosomes: convergent evolution, meiotic adaptations, and genomic analysis. Chromosome Res 20, 579–593.
Mitra S, Srinivasan B, Jansen LET (2020). Stable inheritance of CENP-A chromatin: inner strength versus dynamic control. J Cell Biol 219, e202005099.
Moree B, Meyer CB, Fuller CJ, Straight AF (2011). CENP-C recruits M18BP1 to centromeres to promote CENP-A chromatin assembly. J Cell Biol 194, 855–871.
Moyle MW, Kim T, Hattersley N, Espeut J, Cheerambathur DK, Oegema K, Desai A (2014). A Bub1-Mad1 interaction targets the Mad1-Mad2 complex to unattached kinetochores to initiate the spindle checkpoint. J Cell Biol 204, 647–657.
Musacchio A, Desai A (2017). A molecular view of kinetochore assembly and function. Biology (Basel) 6, 5.
Nardi IK, Zasadzinska E, Stellfox ME, Knippler CM, Foltz DR (2016). Licensing of centromeric chromatin assembly through the Mis18α-Mis18β heterotetramer. Mol Cell 61, 774–787.
Oegema K, Desai A, Rybina S, Kirkham M, Hyman AA (2001). Functional analysis of kinetochore assembly in *Caenorhabditiselegans*. J Cell Biol 153, 1209–1226.
Oegema K, Hyman AA (2006). Cell division. WormBook 1–40.
Ohzeki J, Bergmann JH, Kouprina N, Noskov VN, Nakano M, Kimura H, Earnshaw WC, Larionov V, Masumoto H (2012). Breaking the HAC barrier: histone H3K9 acetyl/methyl balance regulates CENP-A assembly. EMBO J 31, 2391–2402.
Pan D, Walstein K, Take A, Bier D, Kaiser N, Musacchio A (2019). Mechanism of centromere recruitment of the CENP-A chaperone HJURP and its implications for centromere licensing. Nat Commun 10, 4046.
Phansalkar R, Lapierre P, Mellone BG (2012). Evolutionary insights into the role of the essential centromere protein CAL1 in *Drosophila*. Chromosome Res 20, 493–504.
Pidoux AL, Choi ES, Abbott JK, Liu X, Kagansky A, Castillo AG, Hamilton GL, Richardson W, Rappsilber J, He X, Allshire RC (2009). Fission yeast Scm3: a CENP-A receptor required for integrity of subkinetochore chromatin. Mol Cell 33, 299–311.
Prosée RF, Wenda JM, Gabus C, Delaney K, Schwager F, Gotta M, Steiner FA (2020). Trans-generational inheritance of centromere identity requires the CENP-A N-terminal tail in the *C.elegans* maternal germ line. BioRxiv, https://doi.org/10.1101/2020.10.05.325985.
Ravi M, Kwong PN, Menorca RM, Valencia JT, Ramahi JS, Stewart JL, Tran RK, Sundaresan V, Comai L, Chan SW (2010). The rapidly evolving centromere-specific histone has stringent functional requirements in *Arabidopsis thaliana*. Genetics 186, 461–471.
Sanchez-Pulido L, Pidoux AL, Ponting CP, Allshire RC (2009). Common ancestry of the CENP-A chaperones Scm3 and HJURP. Cell 137, 1173–1174.
Shuaib M, Ouararhni K, Dimitrov S, Hamiche A (2010). HJURP binds CENP-A via a highly conserved N-terminal domain and mediates its deposition at centromeres. Proc Natl Acad Sci USA 107, 1349–1354.
Steiner FA, Henikoff S (2014). Holocentromeres are dispersed point centromeres localized at transcription factor hotspots. Elife 3, e02025.
Wang J, Liu X, Dou Z, Chen L, Jiang H, Fu C, Fu G, Liu D, Zhang J, Zhu T, *et al*. (2014). Mitotic regulator Mis18β interacts with and specifies the centromeric assembly of molecular chaperone holliday junction recognition protein (HJURP). J Biol Chem 289, 8326–8336.
Williams JS, Hayashi T, Yanagida M, Russell P (2009). Fission yeast Scm3 mediates stable assembly of Cnp1/CENP-A into centromeric chromatin. Mol Cell 33, 287–298.
Zhang D, Martyniuk CJ, Trudeau VL (2006). SANTA domain: a novel conserved protein module in Eukaryota with potential involvement in chromatin regulation. Bioinformatics 22, 2459–2462.